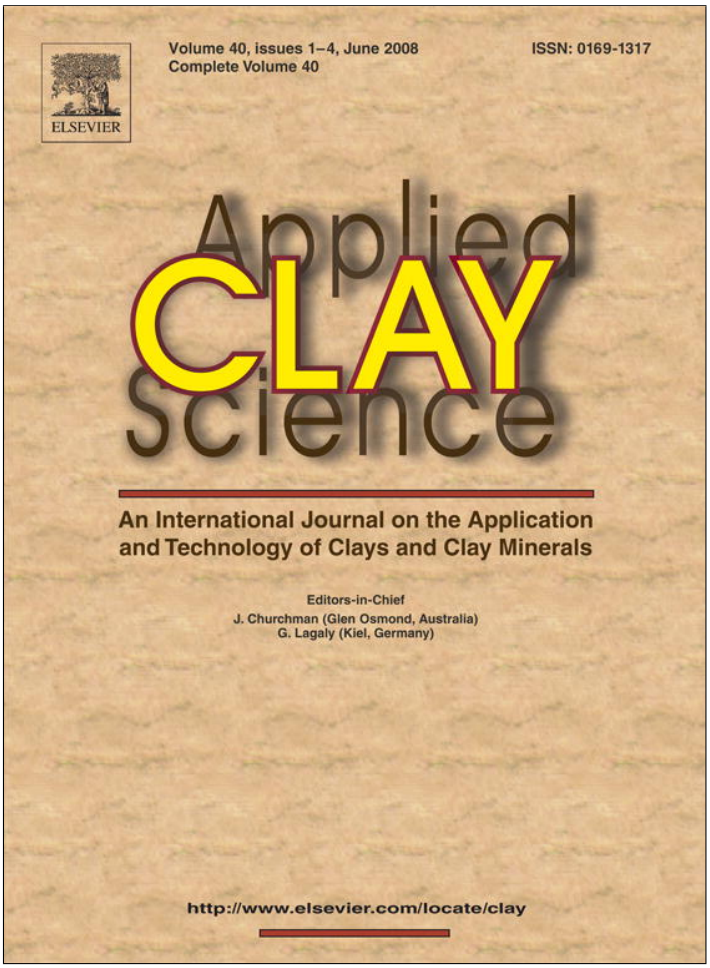

Available online at www.sciencedirect.com
ScienceDirect
Applied Clay Science 40 (2008) 124–142
Applied CLAY Science
www.elsevier.com/locate/clay

The geology and mineralogy of a range of kaolins from the Santa Cruz and Chubut Provinces, Patagonia (Argentina)

Eduardo Dominguez [a], Claudio Iglesias [b], Michele Dondi [c,*]

[a] Departamento de Geología, Universidad Nacional del Sur, San Juan 670, 8000 Bahía Blanca, Argentina
[b] Piedra Grande SA, Dique Florentino Ameghino, Dto. Gaiman, A.P. Bell 569, 9100 Trelew, Chubut, Argentina
[c] CNR-ISTEC, Istituto di Scienza e Tecnologia dei Materiali Ceramici, Via Granarolo 64, 48018 Faenza, Italy

Received 30 May 2005; received in revised form 11 July 2007; accepted 17 July 2007
Available online 7 August 2007

Abstract

In the Santa Cruz and Chubut provinces, Patagonia, Argentina, kaolin deposits were formed by "in situ" alteration of volcaniclastic rocks, such as the Bajo Grande, Chon Aike or Marifil Formations, or by erosion, transportation, and deposition of residual clays in small basins. This paper describes the genesis; geology; mineralogy; major, minor, and trace element geochemistry; grain size distribution; and specific surface area of natural and washed kaolins in an attempt to understand their behavior in the ceramic process. The sedimentary clays of the Baqueró Fm Lower Member, related to the Bajo Grande basement, are kaolinitic–smectitic, very fine-grained, and with a very high specific surface area. The clays related to the Chon Aike or Marifil Fms are kaolinitic, showing intermediate values of specific surface area and a coarser particle size distribution, associated with quite a fine-grained texture. The Baqueró Fm Upper Member received a considerable pyroclastic supply, fostering the development of a fine-grained clay in which kaolinite (±halloysite) with higher values of kaolinite crystal order prevailed. Primary kaolins – derived from weathering of pyroclastic sequences of Chon Aike and Marifil Fms – are coarse-grained, composed of kaolinite+quartz±halloysite and exhibit a very low specific surface area. Alteration of mostly crystalline pyroclastics yielded ordered kaolinite and illite (+halloysite) with a fine particle size distribution and intermediate values of specific surface area. Alteration of mainly vitreous pyroclastics produced halloysite (+kaolinite) with a fine-grained texture and moderately high values of specific surface area. A supergene origin of primary kaolins is inferred on the basis of palaeoclimatic and geochemical evidence that corroborates stable isotopic data. The mineralogy, grain size, and textural characteristics of clays are controlled by parent rock composition (primary kaolins) or by provenance and proximity to source areas (sedimentary kaolins).

Keywords: Clay mineralogy; Kaolin; Particle size distribution; Patagonia; Specific surface area; Weathering

1. Introduction

In the Santa Cruz and Chubut provinces, Patagonia, Argentina, kaolin deposits have been formed by two different processes, either "in situ" alteration of volcaniclastic rocks (primary or residual kaolins) or erosion, transportation, and deposition of residual clays in small continental basins (secondary, sedimentary or *ball clays*). Residual kaolin deposits are found in several Jurassic volcanic rocks, ranging from rhyolites to ignimbrites and tuffs, that were argillized to kaolinite in most cases (Chon Aike, La Matilde or Marifil Formations) or to smectite in others (Bajo Grande Fm) (Cravero and Dominguez, 1992; Dominguez and Murray, 1995). Sedimentary deposits are

* Corresponding author. Fax: +39 0546 46381.
E-mail address: dondi@istec.cnr.it (M. Dondi).

0169-1317/$ - see front matter © 2007 Elsevier B.V. All rights reserved.
doi:10.1016/j.clay.2007.07.009

found in the Cretaceous Baqueró Fm in Santa Cruz and in the Paleocene Salamanca Fm in Chubut.

The Patagonian kaolin deposits have been exploited since 1940 and, at present, ~250,000 t are extracted each year, with the ceramic industry the major end-user. Despite this intensive exploitation, references to the ceramic properties of Patagonia raw materials are scarce. The lithological differences among parent rocks of primary kaolins as well as the distinct influences of erosion areas and the sedimentary clay stratigraphic position imply differences in mineralogy and grain size distribution that should have direct consequences on the ceramic properties of clay raw materials (Worrall, 1975; Powell, 1996).

The objective of this and the associated paper (Dondi et al., 2008) is therefore to seek the interconnections between clay deposit geological features and kaolin ceramic behavior. Even though kaolinite is the major mineral in most deposits, there are significantly different mineralogical assemblages and kaolinite characteristics in the different mines. These features need to be clearly understood in order to manage daily changes during extraction and to fulfil the strict clay type requirements for the ceramic industry (Eichlin, 2001).

The first part of this study herein describes geology, mineralogy, major and trace elements – including one new stable isotopic datum – grain size distribution, and surface area of natural and washed primary and secondary kaolins. The second part of this work (Dondi et al., 2008) deals with technological properties of clays and their behavior in the ceramic process.

A direct relation between primary kaolinite blankets and hydrothermal activity has been assumed, since, in recent years, epithermal Au–Ag mineralizations have been found in Chon Aike and Marifil Fms (Schalamuk et al., 1997). Paleoclimatic evidence and the distribution of trace elements in primary and sedimentary clays – including oxygen and hydrogen isotopes – are considered evidence that favors an origin by weathering.

2. Regional geology

2.1. Santa Cruz Province

In the Santa Cruz province, residual kaolin deposits are found in the Lote 18 area (Fig. 1); similar deposits appear in neighboring areas, such as Lote 8, Lote 19, and Cerro Rubio (Panza et al., 1994; Dominguez and Murray, 1997; Cravero et al., 2001) and other minor locations. These deposits occur in the Jurassic Bahía Laura Group, composed by ignimbrites and rhyolites from Chon Aike Fm and tuffs from La Matilde Fm (Lesta and Ferello, 1972). The Bahía Laura Group unconformably lays over sporadic outcrops of Proterozoic to Eocambric phyllites and schists (Di Persia, 1962), Siluric granites (Palma, 1989), and Permotriassic sediments of La Golondrina and El Tranquilo Fms (Stipanicic and Reig, 1956; Archangelsky, 1959; Arrondo, 1972).

Over the Bahía Laura Group, sedimentary and pyroclastic rocks were deposited in small basins from Upper Jurassic to Lower Cretaceous. These rocks have been mapped as the Bajo Grande Fm (Di Persia, 1957; Lesta, 1969). However, this interpretation is under debate, since for some authors these rocks belong to the Bahía Laura Group (Henchern and Homovic, 1998). The upper part of this sequence is formed by a very fine-grained, vitro-crystalline tuff that has been altered into a smectitic clay.

During Cretaceous, a thick continental sequence – the Baqueró Fm – was sedimented in a fluvial and lacustrine environment over the Chon Aike Group and the Bajo Grande Fm (Archangelsky, 1963). This unit is subdivided into a Lower Member, containing sedimentary clay bodies (Cravero and Dominguez, 1992) and an Upper Member exclusively formed by cinerites and tuffs. The clays are richly fossiliferous.

Several Atlantic Paleocene, Eocene, Oligocene, and Miocene transgressions complete the stratigraphic column.

2.2. Chubut province

In this province, kaolin deposits are found in the lower part of the Río Chubut valley (Fig. 2). Residual deposits are found within the Jurassic Marifil Fm, consisting of rhyolitic vulcanites (Malvicini and Llambías, 1974), that are correlated to the Bahía Laura Group. This unit lays over a Proterozoic Basement composed of gneisses and micaschists intruded by syntectonic granites (Stipanicic and Methol, 1972). In addition, some continental Cretaceous deposits have been described near the Andes far away from kaolin deposits (Chubut Group).

The Paleocene Salamanca Fm, made up of clays, sandstones, and limestones (coquinas) deposited in a coastal and shallow marine environment (Lesta and Ferello, 1972) overlies the Marifil Fm. Sedimentary clay bodies are located close to the erosive contact of the two formations. As in the Santa Cruz province, the stratigraphic sequence ends up with marine deposits from Neogene transgressions.

3. Materials and methods

Fifteen samples were collected in nine active quarries and in two residual argillized areas according to the following criteria: their primary or secondary origin, their relation with

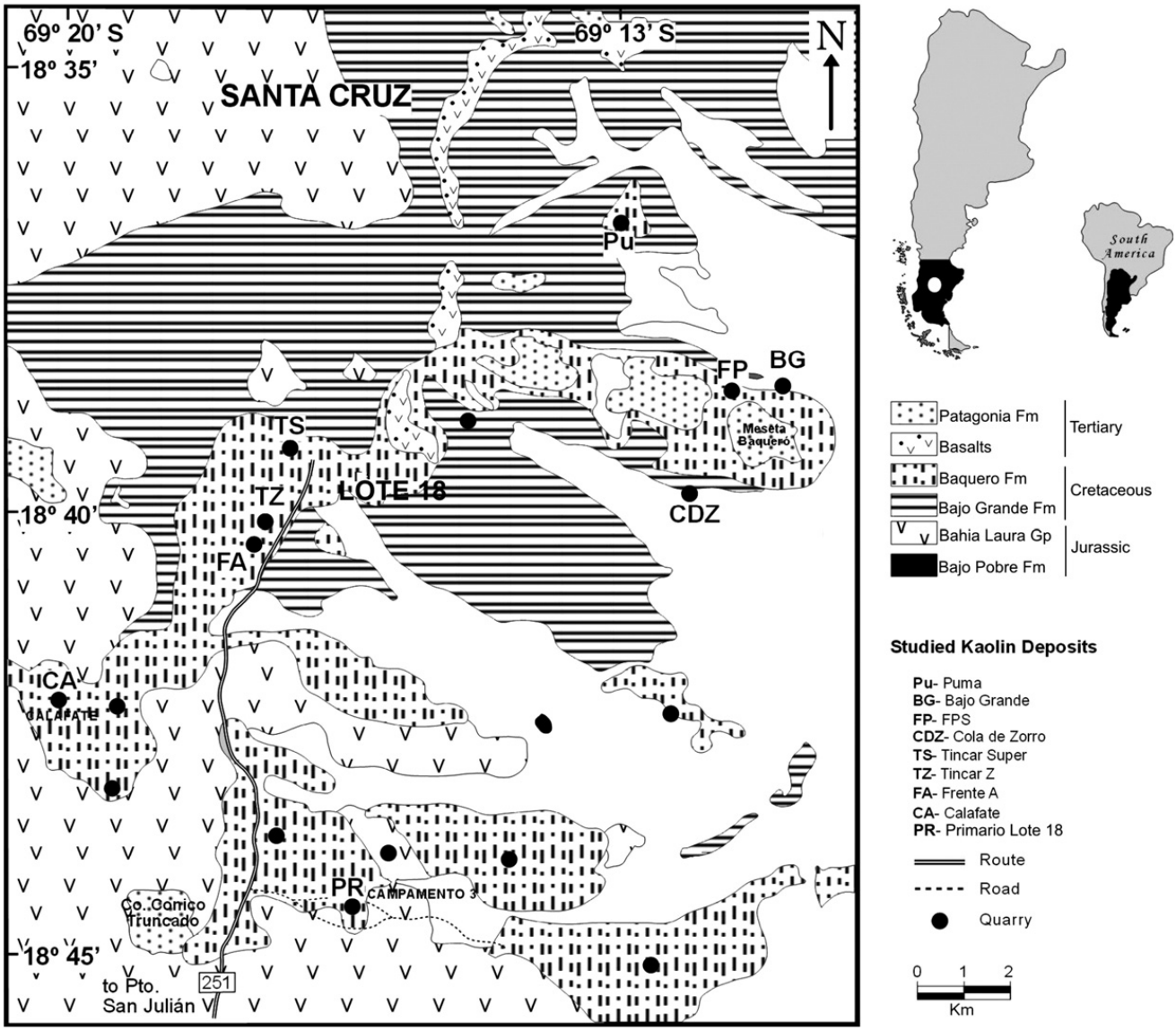

Fig. 1. Geological map of the Lote 18 Santa Cruz kaolin district (modified after Cravero and Dominguez, 1992).

the eroded basement, their position in the sedimentary sequence overlying basement rocks, and the economic significance of the deposits. Moreover, six primary kaolins from the most representative deposits were processed to recover the fine-grained, kaolinite-rich fraction.

In the Santa Cruz province, two distinct depositional sequences of the Baqueró Fm were studied, lying on the Chon Aike Group and the Bajo Grande Fm respectively (Fig. 3 and Table 1). In the Chubut province, three important quarries, operating in the altered volcanic basement of the Marifil Fm, were sampled together with a sedimentary clay of the Salamanca Fm (Fig. 2 and Table 1).

In each quarry, a 60 kg clay sample was taken, crushed, and divided into four equivalent batches. In the case of primary deposits, one batch underwent the industrial processing cycle, consisting in washing, coarser fraction settling, clay-rich suspension separation, filter-pressing and drying.

Clay samples were characterized from mineralogical, geochemical, microstructural, and granulometric viewpoints. Mineralogy was investigated by X-ray powder diffraction performed on randomly oriented specimens – whole rock – and on specimens of the <2μm fraction - extracted by sedimentation according to Stokes' law – using a Rigaku–Denki Geigerflex Max III C diffractometer – $2°2\theta$ min^{-1}, graphite-monochromated Cu K_α radiation. Kaolinite structural order was measured according to Hinckley's (1963) and Stoch's (1974) methods, following the recommendations of Aparicio and Galán (1999) and Guggenheim et al. (2002) on the <2 μm fraction.

The X-ray diffraction patterns were performed on the whole air-dried clay samples as used in the ceramic industry. The illite and interstratified illite/smectite (I/S) were defined on the basis of 10 Å basal reflections. The mineral with sharper 10 Å and 5 Å reflections was considered illite, while that with a wider basal

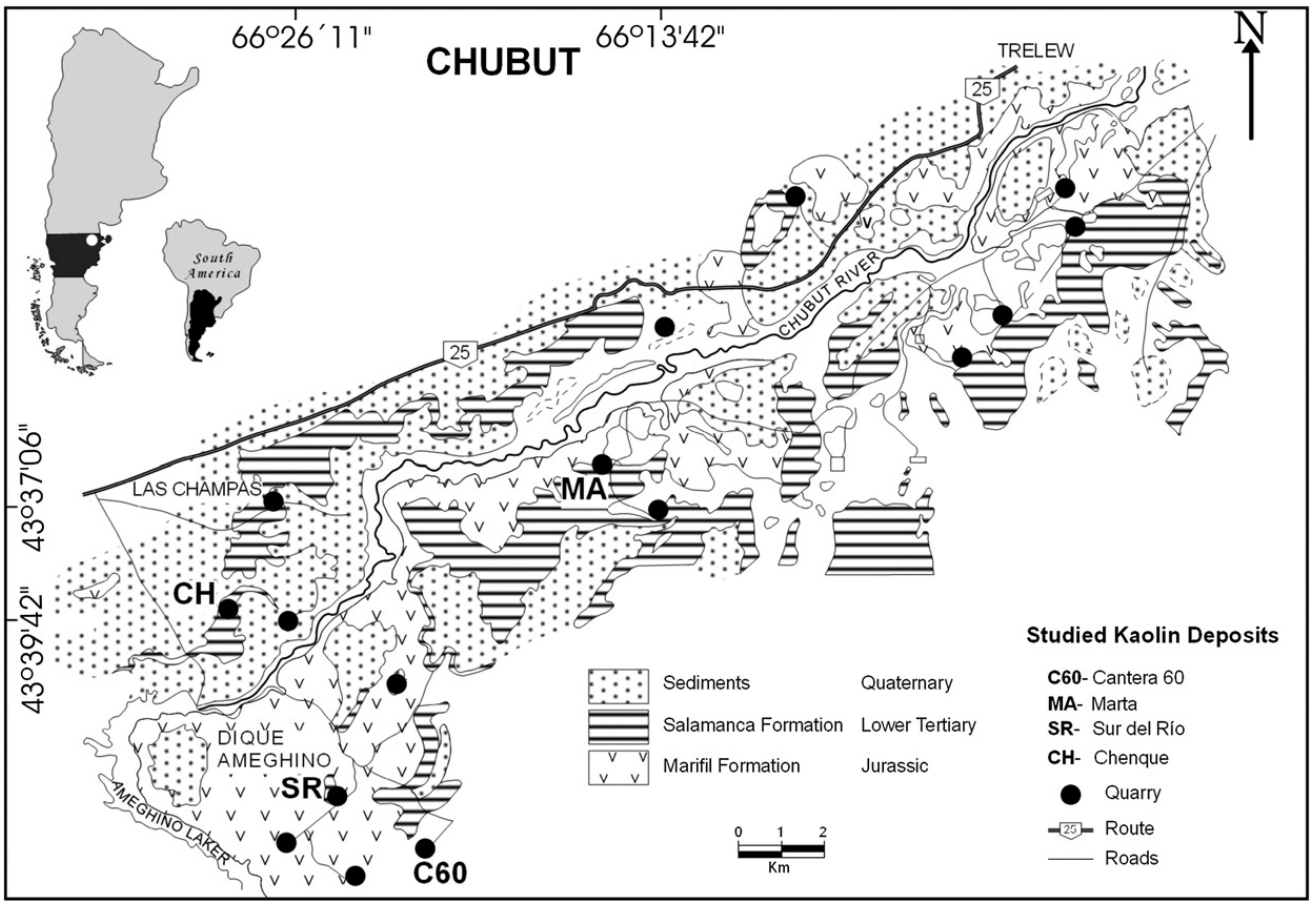

Fig. 2. Geological map of Chubut kaolin district (modified after Dominguez and Murray, 1997).

reflection and a peak located around 11 Å in diffraction patterns from air-dried random <2 μm samples was considered I/S. Both were characterized as illitic materials, since a detailed identification (Srodon and Eberl, 1987) was not performed. The identification method for the <2 μm fraction is shown in Fig. 4 for three selected samples.

Whole rock quantitative mineralogical composition was achieved by both normative calculations and X-ray pattern

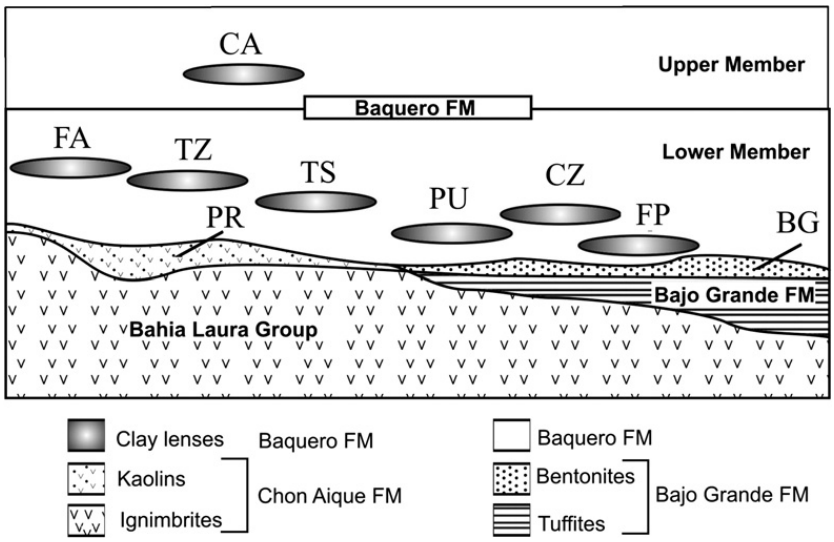

Fig. 3. Depositional sequences in Santa Cruz Province, Patagonia, showing the stratigraphic position of clay deposits. CA: Calafate, FA: Frente A, TZ: Tincar Z, TS: Tincar Super, PR: Primary Lote 18, PU: Puma, CZ: Cola de Zorro, FP: FPS, and BG: Bajo Grande.

Table 1
Genetic and stratigraphic features of the Patagonian kaolins and clays

Deposit	Code	Type	Prov.	Sequence	Formation	Age
Bajo Grande	BG	P	Santa Cruz	Bajo Grande	Bajo Grande	Late Jurassic–Early Cretaceous
FPS	FP	S			Baqueró LM	Lower Cretaceous
Puma	PU	S			Baqueró LM	Lower Cretaceous
Cola de Zorro	CZ	S			Baqueró LM	Lower Cretaceous
Lote 18	PR	P	Santa Cruz	Chon Aike	Chon Aike	Jurassic
Tincar Super	TS	S			Baqueró LM	Lower Cretaceous
Tincar Zeta	TZ	S			Baqueró LM	Lower Cretaceous
Frente A	FA	S			Baqueró LM	Lower Cretaceous
Calafate	CA	S			Baqueró UM	Lower Cretaceous
C60–ILG	IL	P	Chubut		Marifil	Jurassic
C60–RPB	RP	P			Marifil	Jurassic
C60–RF	RF	P			Marifil	Jurassic
Sur del Rio	SR	P			Marifil	Jurassic
Marta	MA	P			Marifil	Jurassic
Chenque	CH	S			Salamanca	Paleocene

P = primary or residual; S = secondary or sedimentary. LM = Lower Member; UM = Upper Member.

interpretation, applying the generalized reference intensity ratio (RIR) and assuming a theoretical composition for kaolinite, quartz, and feldspars as well as a mean composition for illite and smectite. DTA and TGA were simultaneously performed using a Rigaku–Denki analyzer with a heating rate of 10 °C min^{-1} in the 20–1000 °C range.

Whole rock chemical analyses of major, minor, and trace elements (including REE) were performed by Instrumental Neutron Activation Analysis (INAA), Inductively-Coupled Plasma Optical Emission Spectrometry (ICP-OES), and X-ray Fluorescence Spectrometry (XRF). Carbon and sulphur concentrations were determined by IR absorption (Leco CS225, ASTM E 1019).

Microstructure was observed by both scanning electron microscopy (JEOL 35 CF) and transmission electron microscopy (JEOL 100 CX). Small fragments mounted on Cu holders and coated with an Au–Pd alloy were used for SEM, while for TEM water suspensions sprayed on Cu 200 mesh holders and bright field techniques were used. Particle size distribution was measured by X-ray monitoring of gravity sedimentation (Micromeritics Sedigraph 5100, ASTM C 958) and wet sieving of the >100 μm fraction (ASTM C 325). Specific surface area (SSA) was determined by nitrogen absorption using the BET method (Micromeritics FlowSorb II, ASTM C 1069).

4. Geology and mineralogy of kaolin deposits

4.1. Bajo Grande and related basins (Santa Cruz Province)

The residual *Bajo Grande* (BG) deposit is located in the North–East of the Meseta de Baqueró (Fig. 1) where small outcrops of green tuffs are altered into a smectitic clay. Nearly horizontal layers are present in a ~20,000 m^2 quarry, where the alteration depth does not exceed 4 m. BG clay is basically composed of smectite, kaolinite, and quartz, with small amounts of opal CT, feldspar, and iron oxides, thus accounting for its high Fe_2O_3, MgO, and Na_2O content (Tables 2 and 3, Figs. 4 and 5). TGA-DTA results confirm smectite abundance of BG, as it presents the largest weight loss in the 100–150 °C temperature range. SEM images show a typical smectite fine-grained structure – below 0.3 μm – with only a few kaolinite platelets, that are observable under TEM (Fig. 6) together with cuspate shapes attributed to original glass shards. Particle size distribution is the finest among the samples under investigation, while the SSA is unexpectedly low (Table 5).

The *FPS* (FP) quarry, in the Baqueró Fm, is close to BG primary clay outcrops. In this area, the sedimentary formation is composed only of dark gray clays with small sandstone lenses. Just over the erosive contact, rounded agglomerates of BG-type smectite, about 2–3 cm in size, are spread into FP clay. This 6 m-thick body mainly consists of poorly ordered kaolinite, smectite, and quartz (Tables 2 and 3, Fig. 5). The presence of K-feldspar and iron oxy-hydroxides explains the relatively high amounts of K_2O and Fe_2O_3. Crystallite sizes are analoguous to those observed under SEM and TEM for BG, though in this case kaolinite crystals are more abundant than smectite with some cuspate remnants (Fig. 6). FP shows the widest SSA and a very fine particle size distribution, almost entirely below 4 μm (Fig. 7a).

The *Puma (PU)* quarry is located in the northern part of the kaolin district, not far from the contact with the Bajo Grande Fm. The Baqueró Fm is represented by 4 m of conglomerates and sandstones covered by 8 m of dark gray clay with abundant organic carbon, composed of kaolinite, quartz, and an expandable clay mineral, I/S or smectite (Fig. 5). Kaolinite is disordered as indicated by

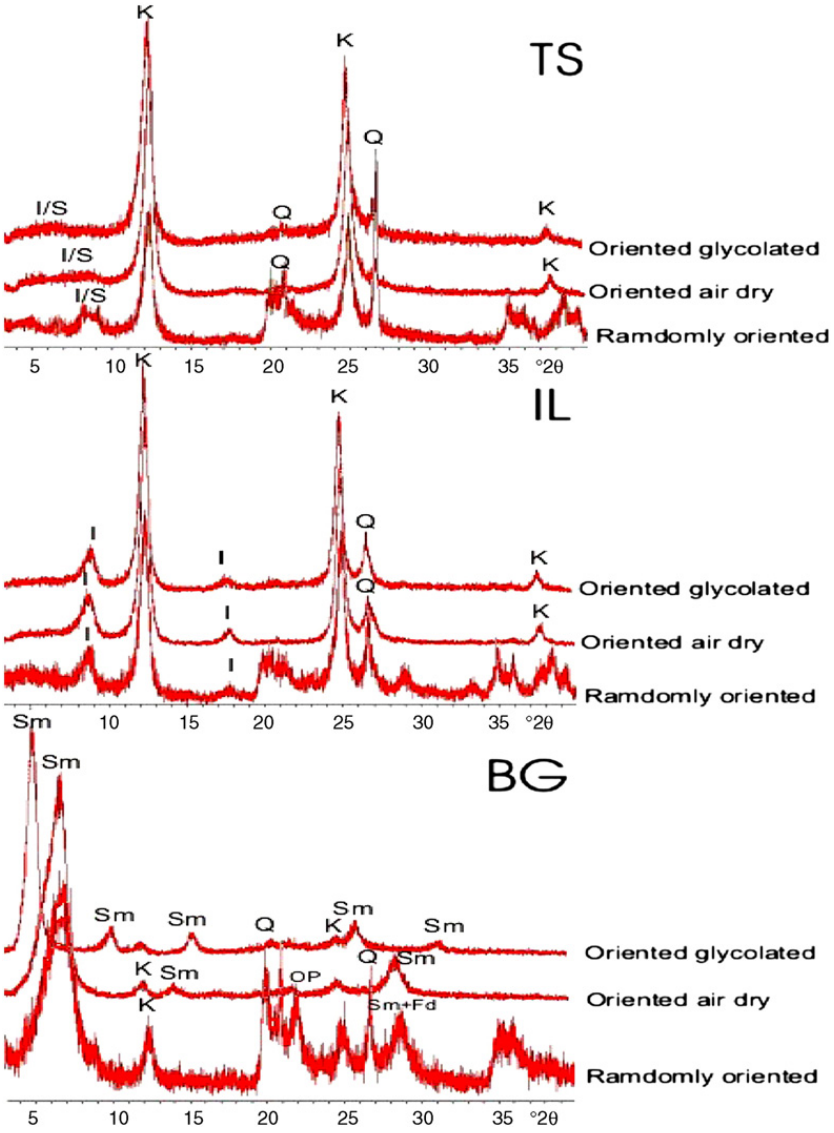

Fig. 4. Identification method on <2 μm clay samples. Sm: Smectite, K: Kaolinite, Q: Quartz, Fd: Feldspars, OP: Opal CT, I: Illite (10 Å non expandable), I/S: (11 Å) expandable.

both the Stoch and Hinckley indices as well as by the fast dehydroxylation rate. These characteristics are common to the whole Bajo Grande sequence (Tables 2 and 4). Moreover, kaolinite crystals exhibit an edge-to-face arrangement with irregular outlines and grain size below 1 μm, similar to FP, except for the very fine-grained smectite being absent at PU (Fig. 6). Grain size distribution is very fine and SSA is high (Fig. 7a).

The *Cola de Zorro (CZ)* sedimentary deposit is located at the SE border of the Baqueró Meseta on a ~7000 m^2 area. In this quarry, developed in the Baqueró Fm, clay layers are horizontal and about 5 m thick. The clay is composed of kaolinite, quartz, and traces of illite-I/S (Tables 2 and 3, Fig. 5) with a rather high value of SSA and a particle size distribution similar to PU (Fig. 7a): small kaolinite platelets with edge-to-face arrangement and rounded morphology (Fig. 6).

4.2. Chon Aike and related basins (Santa Cruz Province)

The primary deposit of *Lote 18* (PR) is about 3 km NE of Conico Truncado hill, where the Baqueró Fm lays over residual kaolinized volcanic breccias. It is composed of quartz and kaolinite with illite traces (Tables 2 and 4, Fig. 8) resulting in a silica-rich composition, almost completely depleted of other components. This sample is dominated by the sandy–silty fraction and has a very low clay fraction and SSA. The alteration extent is unknown, although in Lote 8 it reaches a 6 m depth on average (Dominguez and Murray, 1997). From the microstructural viewpoint, the

Table 2
Mineralogical composition (wt.%) of primary kaolins (P), sedimentary clays (S) and beneficiated products (B)

Deposit	Type	Ka	Hy	I/S	Sm	Qz	Fd	Ac	HI	SI
BG	P	15			59	15	3	8		2.12
FP	S	37			28	23	4	8	0.33	1.60
PU	S	49			12	33	2	4	0.18	1.31
CZ	S	48		3		39	2	8	0.45	1.23
PR	P	29		2		68		1	1.75	0.46
TS	S	52		9		34	2	3	0.37	2.28
TZ	S	43		8		46		3	0.40	1.18
FA	S	50		9		37	1	3	0.64	1.11
CA	S	65	*	tr.		27		8	0.92	0.81
IL	P	28	*	15		53	1	3	0.61	1.09
RP	P	31	**			44	21	4	0.64	0.93
RF	P	35	***			52	7	6	0.46	1.09
SR	P	32	**	5		58		5	0.50	0.97
MA	P	35	*	17		44	2	2	0.79	1.05
CH	S	49	(*)	9		33	5	4	0.51	1.13
PRL	B	28		2		69		1	1.70	0.50
RPL	B	68	**	15		14	1	2	0.69	0.95
ILL	B	63	*	3		31	1	2	0.70	0.81
RFL	B	70	***	3		23	1	3	0.51	1.02
SRL	B	63	**	17		18	1	1	0.45	0.95
MAL	B	57	*	12		29		2	0.73	1.11

Ka: kaolinite, Hy: halloysite, I/S: illite and illite-smectite interstratified, Sm: smectite, Fd: feldspars, Ac: accessories (mainly iron oxi-hydroxides). Kaolinite 'crystallinity': Hinckley's (HI) and Stoch's (SI) indices.
Asterisks indicate the relative abundance of halloysite as estimated by SEM and TEM analyses.

main feature is the occurrence of kaolinite platelets larger than 5 μm arranged as worm-like booklets larger than 7 μm; this texture occupies open spaces (Fig. 9).

The *Tincar Super* (TS) quarry operates over a 7 m clay layer on a ~60,000 m^2 surface in the Baqueró Fm. The clay is white and massive with some quartz grains and frequently contains plant fossils without carbon. The composition is dominated by poorly ordered kaolinite with quartz and some illite (I/S). The kaolinite crystals have irregular boundaries and a face-to-face arrangement, with a crystallite size of 1-2 μm (Tables 2 and 4, Fig. 9). Such a crystallite size is in agreement with the predominance of the <2μm fraction; however an abundant silty fraction is also present (Fig. 7b) thus justifying the low SSA values.

The *Tincar Zeta* (TZ) and *Frente A* (FA) quarries are operating over a ~80,000 m^2 area located 3 km south of TS, at the top of the Lower Member of the Baqueró Fm. These two deposits are interfingered and the 8 m thick clay layer is massive, interbedded between conglomerates and sands, with poorly defined strata and a whitish (FA) or grayish color (TZ). Organic matter content, due to fossil plant remains, varies considerably at different exploitation levels, being on the whole around 0.1% (Table 3). These clays are composed of kaolinite and quartz, with trace amounts of illite (I/S) shown in Table 2 and Fig. 8. Kaolinite has a degree of structural order higher than in the Bajo Grande sequence, as confirmed by both Hinckley and Stoch indices and also the slower dehydroxylation rates (Table 4). The kaolinite platelets are 2-3 μm with a face-to-face arrangement (TZ) or smaller than 2 μm with mostly face-to-face arrangements (FA), though some edge-to-face textures are observable (Fig. 9). Particle size curves and SSA can be compared to those at TS (Fig. 7b and Table 5).

The *Calafate* (CA) quarry is exploiting a 3 m thick horizontal layer of massive gray clay with rounded altered lapilli clasts, located 7 km Southwest of TZ. This deposit probably belongs to the Upper Member of the Baqueró Fm due to the abundance of pyroclastic supply. The clay is composed of well-ordered kaolinite prevailing over quartz and traces of illite (I/S) and iron oxy-hydroxides (Tables 2 and 3, Fig. 4). SEM shows an open texture of very fine grains (<1 μm) and TEM shows hexagonal kaolinite crystals associated with some fibers, attributable to illite (Fig. 9). These observations satisfactorily match a clay fraction predominance and a relatively large SSA (Fig. 7b, Table 5).

4.3. Chubut Province deposits

Cantera 60 is a quarry operating over a ~20,000 m^2 area in which a widespread alteration of volcaniclastic rocks has taken place in the Marifil Fm. Three argillized lithological units have been identified: a coarse lithic ignimbrite (IL), a porphyric biotitic ignimbrite (RP), and a vitreous, fluidal, deeply kaolinized rhyolite (RF). The color of these primary rocks is a uniform violet-to-reddish white. Alteration is progressively reduced downward and vanishes between 8 and 12 m from the surface. The deepest alteration seems to be related to a fault zone that puts the three volcanic units into contact. IL is composed of quartz, kaolinite, and illite, arranged in open textures with short kaolinite stacks made up of coarse platelets (3–4 μm) with well defined borders and some rare fibers, attributed to halloysite (Tables 2 and 3, Fig. 11). RP has a different degree of alteration, with abundant residual feldspars, but biotite is totally altered. It has an open texture with short, poorly developed kaolinite stacks, associated with short halloysite fibers and corroded feldspars (SEM images, Fig. 11); TEM examination reveals well defined, 3–4 μm-long kaolinite platelets and halloysite fibers (Fig. 11). RF shows deeper kaolinization with a small amount of feldspars. Its open texture is characterized by abundant 5μm-long

Table 3
Chemical composition of the Patagonian kaolins and clays

Sample		BG	FP	PU	CZ	PR	TS	TZ	FA	CA	IL	RP	RF	SR	MA	CH
SiO_2	wt.%	55.27	58.22	62.97	65.69	83.48	64.55	70.06	65.53	57.64	74.71	72.31	73.56	77.48	71.21	64.72
TiO_2	wt.%	0.35	0.61	0.66	0.47	0.09	0.48	0.42	0.50	0.48	0.23	0.22	0.22	0.16	0.36	0.32
Al_2O_3	wt.%	19.02	21.50	22.19	21.14	11.70	22.94	19.20	22.41	25.93	15.51	16.22	15.92	15.08	18.69	22.94
Fe_2O_3	wt.%	3.62	3.34	1.26	1.44	0.23	0.83	0.84	0.87	3.31	1.34	1.51	1.46	0.59	1.27	0.99
MnO	wt.%	0.336	0.096	0.008	0.016	0.001	0.004	0.004	0.005	0.005	0.038	0.033	0.024	0.011	0.042	0.030
MgO	wt.%	1.32	0.54	0.26	0.31	0.02	0.23	0.20	0.23	0.12	0.17	0.04	0.06	0.09	0.20	0.26
CaO	wt.%	0.83	0.56	0.31	0.25	0.05	0.25	0.20	0.19	0.18	0.12	0.05	0.14	0.10	0.14	0.07
Na_2O	wt.%	1.14	0.35	0.09	<0.01	<0.01	<0.01	<0.01	<0.01	0.06	0.13	0.73	0.58	<0.01	<0.01	0.59
K_2O	wt.%	0.54	1.24	0.56	0.57	0.12	0.63	0.60	0.88	0.21	1.09	2.54	0.29	0.61	1.32	0.70
P_2O_5	wt.%	0.04	0.03	0.02	0.03	0.03	0.03	0.03	0.04	0.06	0.02	0.03	0.02	0.03	0.03	0.03
C	wt.%	0.06	0.14	0.27	0.03	<0.01	0.06	0.09	0.11	0.06	0.04	0.02	0.05	0.03	0.03	0.04
L.o.I.	wt.%	16.81	13.50	10.89	10.28	4.54	9.87	8.52	9.58	11.91	5.98	5.89	7.40	5.93	6.92	9.48
Ag	ppm	<0.3	0.8	0.7	1.0	0.4	1.1	1.4	0.9	0.8	1.0	<0.3	0.5	<0.3	0.4	0.4
As	ppm	16	20	21	25	35	30	19	27	42	3	9	10	4	8	4
Au	ppb	1	2	5	5	3	16	3	3	<1	<2	<2	<2	2	<1	<2
Ba	ppm	742	210	126	138	60	93	152	95	194	70	168	23	40	13	74
Be	ppm	3	3	3	3	2	3	3	3	3	4	3	2	2	3	2
Bi	ppm	<2	<2	<2	<2	<2	<2	<2	<2	<2	<2	<2	<2	<2	<2	<2
Br	ppm	8	4	19	7	<0.5	17	16	2	9	<0.5	<0.5	1	1	<0.5	2
Cd	ppm	0.5	0.8	0.5	0.7	<0.3	0.7	1.0	<0.3	0.6	0.7	0.4	0.6	0.3	0.4	0.3
Co	ppm	27	11	4	8	2	6	7	3	8	1	1	1	1	1	2
Cr	ppm	12	16	16	14	50	23	23	25	13	6	3	3	19	14	9
Cs	ppm	34	54	36	31	10	35	28	28	7	6	2	2	15	4	18
Cu	ppm	3	17	16	11	10	23	8	16	14	5	6	4	2	2	7
Hf	ppm	6	7	7	7	4	6	6	7	12	7	5	6	7	12	7
Hg	ppm	<1	<1	<1	<1	<1	<1	<1	<1	<1	<1	<1	<1	<1	<1	<1
Ir	ppb	<1	<1	<1	<1	<1	<1	<1	<1	<1	<2	<2	<2	<1	<1	<2
Mo	ppm	12	<2	4	<2	8	<2	<2	5	4	3	2	4	<2	<2	<2
Nb	ppm	15	8	18	17	<1	16	3	15	8	n.d.	n.d.	n.d.	10	13	n.d.
Ni	ppm	4	7	7	8	39	11	11	7	4	4	3	3	3	3	4
Pb	ppm	39	57	62	59	25	70	60	63	34	20	23	33	12	11	39
Rb	ppm	50	100	60	63	15	74	70	75	19	133	94	18	64	90	88
S	ppm	590	70	90	100	170	40	40	70	110	180	430	440	150	110	430
Sb	ppm	2	6	13	14	41	12	10	13	7	1	1	1	1	<0.1	1
Sc	ppm	12	15	13	13	4	16	10	16	20	5	4	5	5	8	8
Se	ppm	<0.8	<0.6	<0.7	3	<0.7	<0.7	<0.6	<0.8	1	<0.5	<0.5	<0.5	<0.6	<0.7	<0.5
Sr	ppm	140	58	35	35	14	25	28	23	23	11	9	11	10	10	18
Ta	ppm	<0.3	1.7	1.8	1.5	1.4	1.2	1.3	1.3	1.7	1.8	1.7	1.8	2.4	2.2	1.7
Th	ppm	24	23	21	23	14	25	19	22	31	31	24	30	41	34	33
U	ppm	5	8	6	6	3	8	15	6	7	4	4	4	3	4	15
V	ppm	31	61	59	42	<5	65	38	60	35	11	34	46	22	70	21
W	ppm	27	19	14	9	7	15	13	14	13	1	4	3	2	2	1
Y	ppm	38	40	33	42	11	41	26	54	86	25	20	24	19	24	36
Zn	ppm	92	87	79	124	12	115	119	52	29	50	32	23	21	49	53
Zr	ppm	197	190	195	179	96	144	158	186	371	262	160	170	160	327	171
La	ppm	143.7	32.5	24.7	37.7	25.7	42.0	20.6	65.7	41.2	46.4	66.7	73.4	60.0	55.0	55.4
Ce	ppm	261.9	69.3	45.9	74.7	28.8	85.5	36.9	131.4	80.1	78.0	96.0	123.0	106.2	84.0	140.0
Nd	ppm	103.0	32.0	24.0	38.0	6.0	40.0	18.0	70.0	39.0	35.0	47.0	55.0	39.0	37.0	50.0
Sm	ppm	16.1	5.9	5.2	7.3	0.6	7.3	3.7	13.0	8.4	5.2	7.8	8.4	5.1	5.0	9.8
Eu	ppm	2.7	1.2	1.0	1.3	<0.1	1.3	0.8	2.4	1.8	0.6	1.0	0.9	0.7	0.7	1.5
Tb	ppm	1.8	1.4	0.8	1.4	<0.1	1.4	0.8	2.2	2.1	0.8	0.9	1.3	0.6	1.0	1.6
Yb	ppm	3.2	4.4	3.8	4.9	2.0	4.4	4.5	5.9	9.2	3.9	3.1	3.6	3.0	4.6	5.6
Lu	ppm	0.5	0.6	0.6	0.7	0.3	0.7	0.6	0.9	1.4	0.6	0.5	0.5	0.5	0.7	0.8

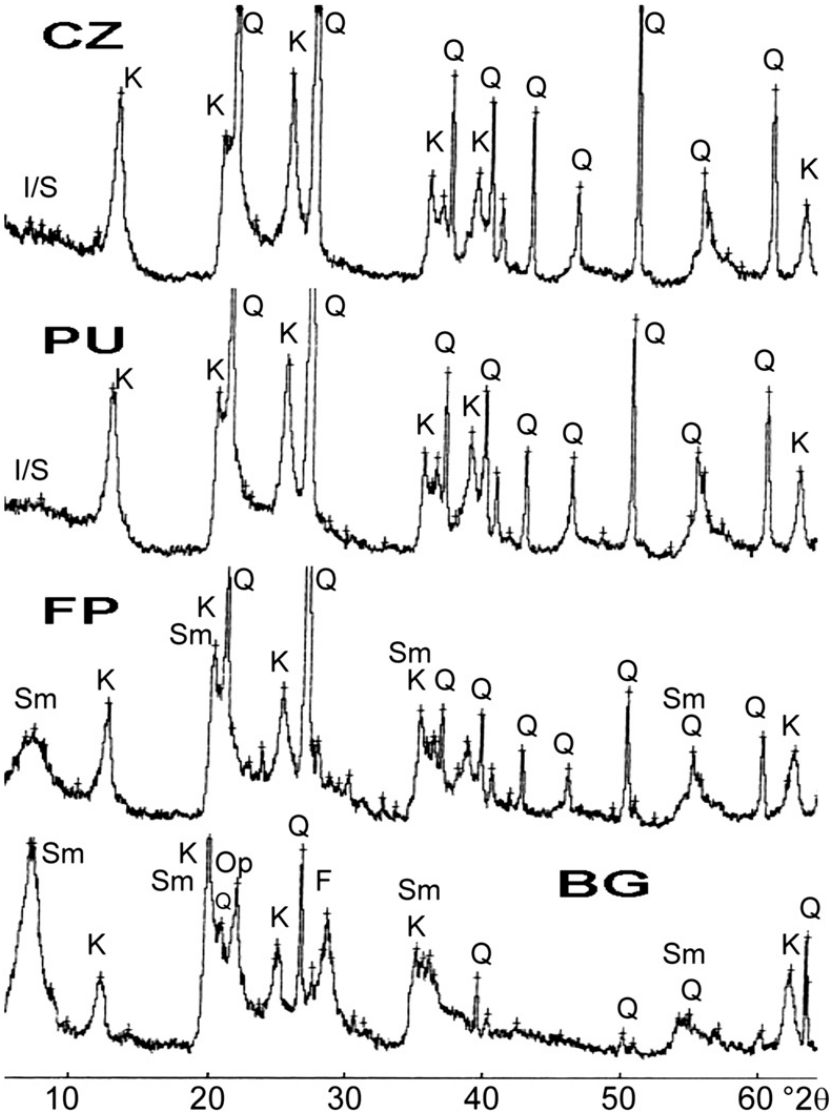

Fig. 5. X-ray diffraction patterns of randomly oriented whole rock clays in Bajo Grande sequence, Santa Cruz Province. Q: Quartz, F: Feldspar, K: Kaolinite, Sm: Smectite, I-I/S: Illitic materials.

halloysite fibers (>70%) scattered over scarce and well-formed 3–4 μm kaolinite platelets (Fig. 11). In these primary deposits, the degree of order of kaolinite is higher than in the sedimentary clays of the Santa Cruz province, except for the CA sample. The sand and silt fractions are abundant, especially in RF and RP (Fig. 7c). Specific surface area is accordingly low, however, the occurrence of illite or halloysite, in IL and RF respectively, increases SSA.

The *Sur del Rio* (*SR*) quarry is developed in an ovoid area of ~500,000 m^2 located on the right bank of Chubut river. Kaolinization reaches a depth of 10 m in a coarse-grained volcanic breccia of the Marifil Fm. In the lowermost levels the deposit is richer in illite (I/S) and iron oxy-hydroxides. Coloration is white in surface samples, becoming more reddish in depth. This kaolin consists of quartz which predominates over kaolinite, plus some illite (I/S) showed in Fig. 10. An open texture, featured by poorly defined kaolinite stacks surrounded by halloysite fibers (>30%), is observed under SEM, while under TEM the kaolinite platelets have well defined hexagonal outlines (3–4 μm) and halloysite has tubular shapes (Fig. 11). Particle size distribution and SSA are close to those of RP (Table 5, Fig. 7c).

In the *Marta* (*MA*) deposit, located 3 km North of C60 and occurring in a circular area of about 10,000 m^2, almost horizontal yellowish white tuff layers of the Marifil Fm have been kaolinized to a depth of 6 m from the surface. The deposit consists basically of quartz, kaolinite, and illite (Tables 2, Fig. 10). MA shows an open texture characterized by fine-grained kaolinite

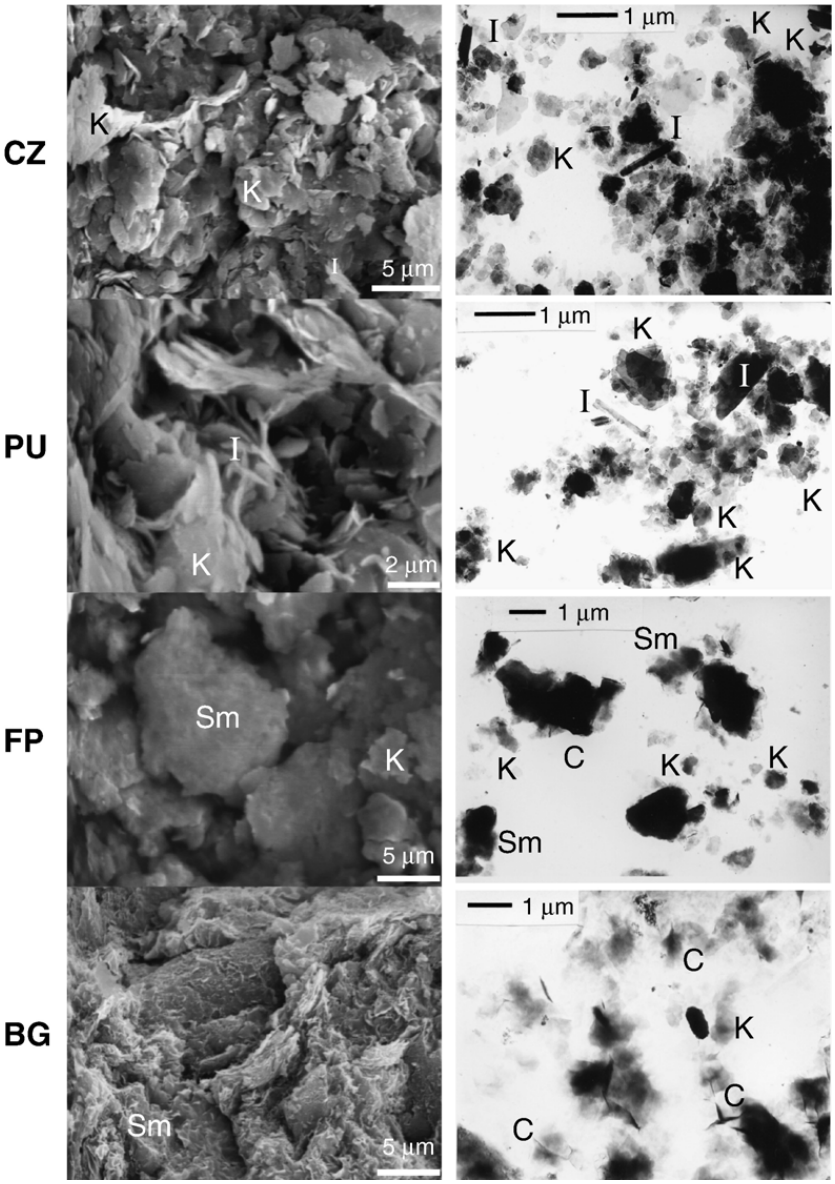

Fig. 6. SEM and TEM micrographs of clays from Bajo Grande sequence (Santa Cruz). K: Kaolinite, Sm: Smectite, I: Illitic materials, C: Smectite pseudomorph of cuspate glass shard shapes.

associated to some fibers (SEM). Under TEM, kaolinite platelets are seen (Fig. 11), whereas the <2 µm fibers may be attributed to halloysite (tubular forms) and illite (wider planar shapes). These features match both the degree of order of kaolinite and particle size distribution, clearly finer than that of the other primary kaolins (Fig. 7c).

In the *Chenque* (CH) sedimentary deposit, pertaining to the Salamanca Fm, a 600 m long front is exploited. The 8 m thick clay body, filling an eroded palaeovalley in Marifil Fm volcanics, has a massive texture and a light gray color with some yellow-reddish layers. The clay consists of quartz, kaolinite, and minor illite (I/S) and feldspars (Table 2, Fig. 10). Kaolinite crystals have a face-to-face arrangement and locally form open booklets. In certain places, some fibers are visible. Under TEM, kaolinite platelets do not have well-defined outlines, while fibers can be ascribed, according to their morphology, to illite and/or halloysite (Fig. 11). Particle size distribution, SSA, and degree of order of kaolinite are similar to those of other sedimentary clays, especially those from the Chon Aike Sequence (Fig. 7c).

5. Discussion

5.1. Genesis of primary kaolins

Primary deposits developed in the Chon Aike Fm and Marifil Fm do not show any strong structural

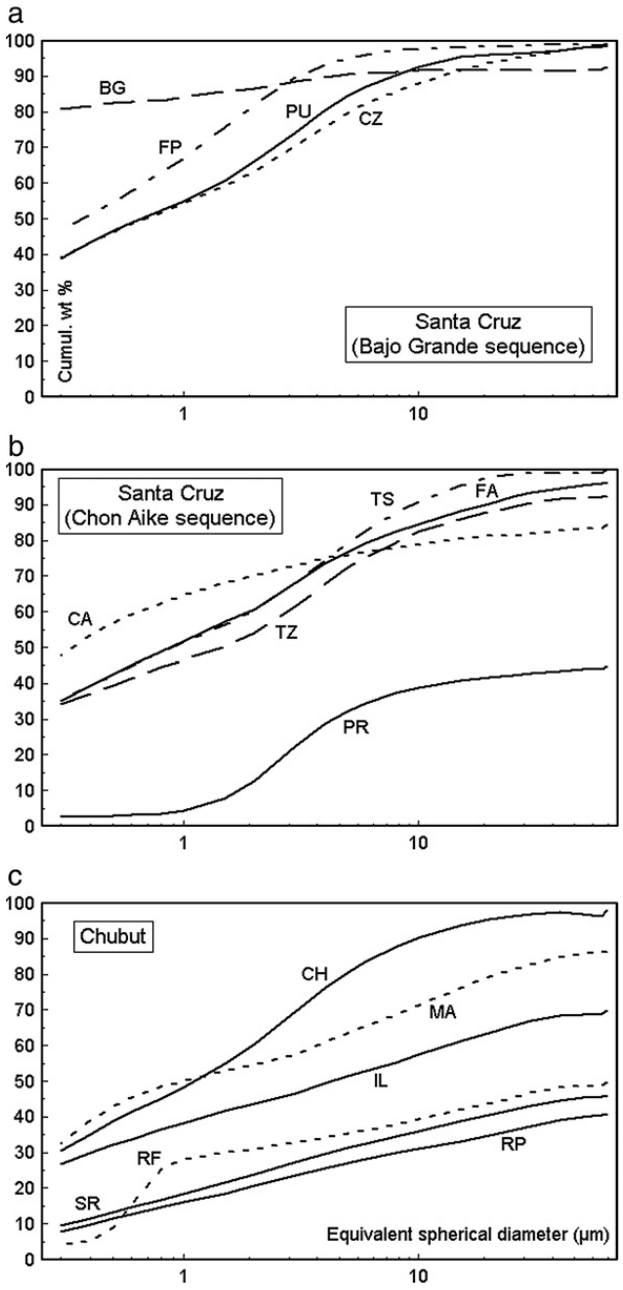

Fig. 7. Particle size distribution of the clays from the Bajo Grande sequence (a), the Chon Aike sequence (b) and the kaolins from Chubut province (c).

control. In contrast, the kaolinized areas have a wide horizontal extension (>1500 m), limited thickness (at most 8–12 m) and a downward decreasing degree of alteration. All deposits occur in the uppermost part of the volcanic sequence and appear to be linked to the unconformity with the overlaying sedimentary units. The mineralogical composition (kaolinite+quartz+feldspars+Fe-oxyhydroxides±halloysite±illite) is inconclusive about a weathering versus hydrothermal genesis.

In the La Matilde Fm (Lesta and Ferello, 1972), the abundant fossil content indicates a warm humid climate in a continental palustrine–fluvial environment (De Barrio et al., 1999). In the case of the Bajo Grande Fm, the smectitization of vitroclastic tuffs may be interpreted as a consequence of a fast alteration process in a subaqueous environment. In the Baqueró Fm, clays are richly fossiliferous, especially containing gymnosperms and angiosperms, indicating a temperate-warm climate (Archangelsky, 1967; Romero and Archangelsky, 1986; Caranza, 1988). The Salamanca Fm was deposited under a warm and humid climate, because the sandstones contain abundant silicified fossil trunks and fossil leaves (Sacomanni and Panza, 1998).

Significantly, both isotopic results (Murray and Janssen, 1984; Cravero et al., 1991; Cravero and Dominguez, 1992; Dominguez and Murray, 1995) and palaeoclimatic conditions point towards a weathering origin for primary kaolinization. A new stable isotopic determination on kaolinite (IL sample) gave $\delta^{18}O$ 13.4 (‰) and δD −85 (‰) compatible with a supergenic-weathering origin (Iglesias, 2005).

Trace element composition was used for the distinction between hypogene and supergene kaolinization mechanisms; in particular, Dill et al. (1997, 2000) applied both the P_2O_5 versus SO_3 and the (Ce+Y+La) versus (Ba+Sr) plots successfully. The Ba+Sr and

Table 4
Thermal behaviour of the Patagonian kaolins and sedimentary clays

	Endothermal peaks	Reaction rate	Exothermal peak	Weight loss (%)	
	°C	% min^{-1}	°C	200–300 °C	1000 °C
BG	150*, 555, 700	1.50	950	10.0 (250)	15.6
FP	145*, 570**	0.50*, 0.75**	975	6.5 (300)	13.2
PU	130, 568*	0.76	960	3.1 (300)	11.3
CZ	120, 565*	0.75	960	3.5 (300)	11.4
PR	555-572	0.20	990	0.8 (300)	4.4
TS	120, 570*	0.53	980	2.5 (300)	10.1
TZ	120, 570*	0.50	970	2.1 (300)	8.6
FA	120, 575*	0.80	980	2.1 (300)	9.6
CA	120, 320, 580*	1.00	970	2.8 (300)	12.0
IL	105, 562*	0.45	980	1.7 (300)	6.9
RP	110, 565*	0.43	980	1.5 (300)	7.0
RF	560*	0.50	990	2.1 (300)	8.8
SR	290, 558*		990	1.9 (300)	7.3
MA	105, 570*	0.60	980	1.4 (300)	7.3
CH	130, 570*	0.73	970	2.8 (300)	11.0

The reaction rate is referred to the endothermal peak with asterisk.

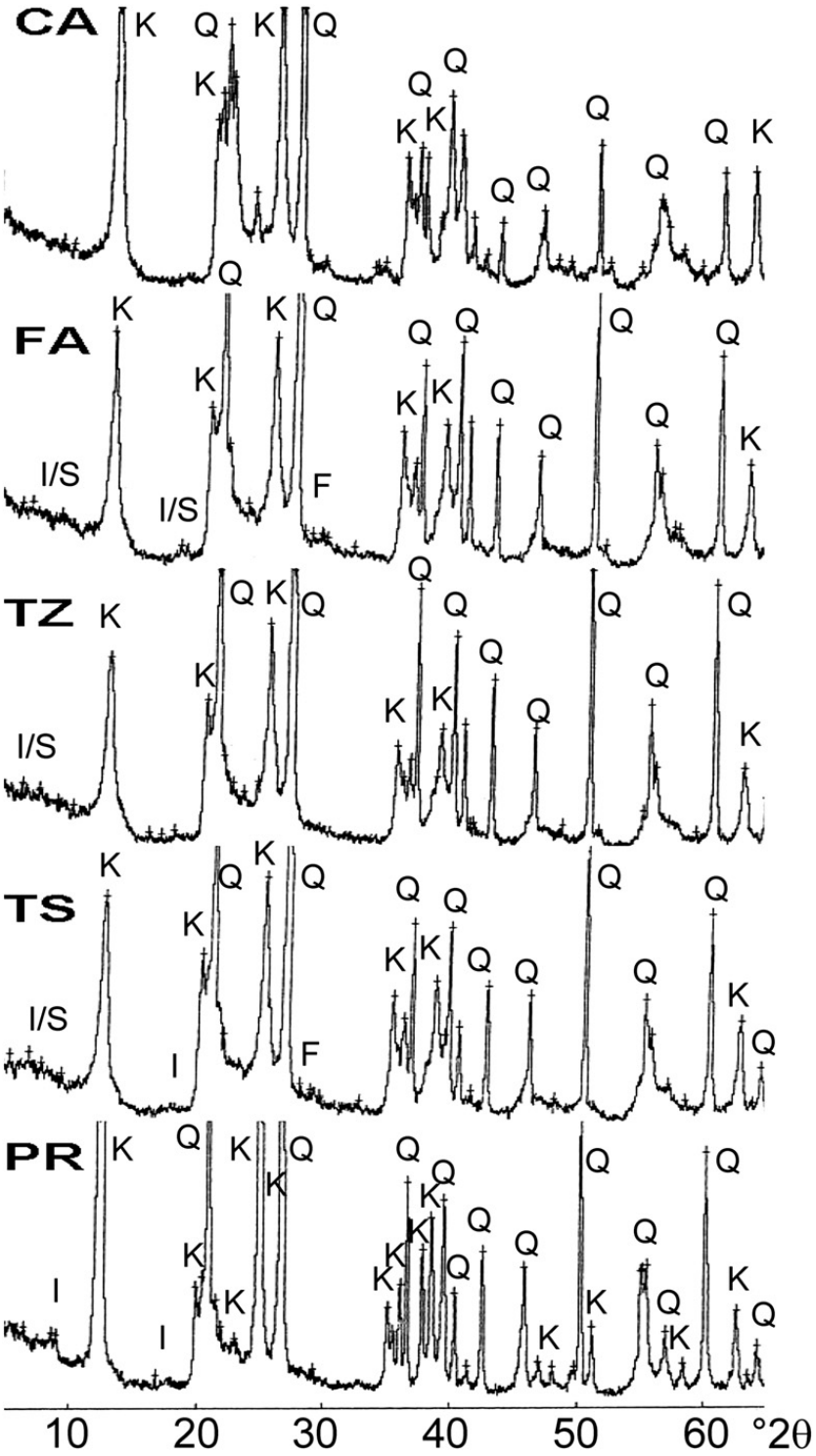

Fig. 8. X-ray diffraction patterns of randomly oriented whole rock clays in the Chon Aike sequence (Santa Cruz). Q: Quartz, K: Kaolinite, F: Feldspar, I-I/S: Illitic materials.

SO_3 contents are useful indicators of hydrothermal activity in Patagonia since the most frequent gangue minerals in epithermal lodes are pyrite and barite. These diagrams would indicate a supergene origin (Fig. 12). Moreover, the contents of Ag, As, Au, Ba, Hg, Mo, Pb, S, Sb, Sr, Ta, and Zn can be taken as geochemical indicators of gold-silver mineralizations. In kaolin deposits, these trace elements are not significantly high in both primary and sedimentary clays (Table 3 and Fig. 13).

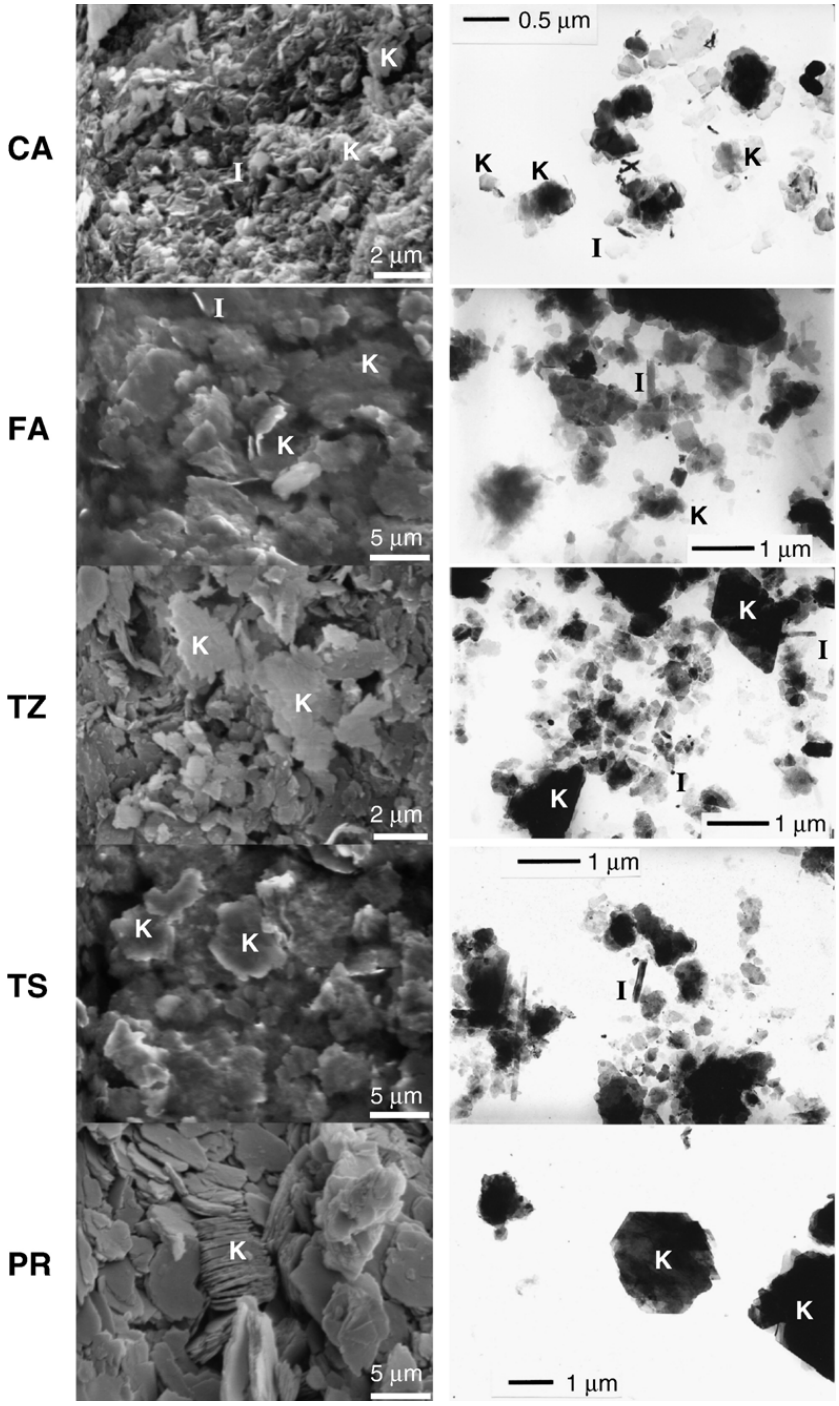

Fig. 9. SEM and TEM micrographs of kaolins and clays from the Chon Aike sequence (Santa Cruz). K: Kaolinite, I: Illitic materials.

5.2. Influence of provenance and sedimentation processes

In the Santa Cruz province, two interlinked basins inside the Baqueró Fm can be distinguished, according to their relation with the eroded basement (Chon Aike or Bajo Grande Fms) and the stratigraphic position of sedimentary clays. In the former basin, where sedimentary deposits FP, PU and CZ are found, the main source is the Bajo Grande basement, whose smectitic contribution is evident in the lower clay layers, whereas the influence from the Chon Aike basement is of lesser importance. The sediment composition changes upwards, so that the upper stratigraphic levels do not contain smectite and have low concentrations of trace elements (e.g. Co, W) compared to Bajo Grande Fm.

Table 5
Particle size distribution and specific surface area (SSA) of kaolins, clays and beneficiated products. Φ_{50}: median particle diameter

	Φ_{50}	Particle fraction (wt.%)							SSA
	μm	>63 μm	4-63 μm	<4 μm	>20 μm	2-20 μm	<2 μm	<0.3 μm	m^2/g
BG	<0.30	7.5	4.1	88.4	8.4	5.9	85.7	80.9	31.7
FP	0.37	0.8	9.6	89.6	2.0	22.4	75.6	46.9	44.5
PU	0.67	1.7	24.1	74.2	4.7	34.7	60.6	38.7	28.0
CZ	0.68	1.2	28.4	70.4	8.2	32.5	59.3	39.0	24.3
PR	>63	55.2	22.4	22.4	59.1	33.0	7.9	2.5	3.1
TS	0.88	0.1	31.7	68.2	4.5	39.1	56.4	35.6	22.7
TZ	1.47	7.6	31.0	61.4	14.0	35.8	50.2	34.2	21.2
FA	0.88	3.7	28.3	68.0	21.9	21.0	57.1	35.0	21.7
CA	0.33	15.6	11.5	72.9	19.6	12.3	68.1	47.8	25.6
IL	4.29	30.2	23.2	46.6	38.7	19.6	41.7	26.6	13.3
RP	>63	59.2	17.2	23.6	67.0	14.5	18.5	7.9	7.4
RF	63.5	49.8	17.5	32.7	58.1	11.9	30.0	4.0	13.1
SR	>63	54.0	18.8	27.2	61.3	17.2	21.5	9.5	8.8
MA	1.00	13.7	28.8	57.5	23.9	23.2	52.9	32.6	14.2
CH	1.11	2.0	28.4	69.6	6.2	38.9	54.9	30.6	21.3
PRL	2.39	0.1	22.8	77.1	1.3	58.8	39.9	5.8	5.8
ILL	0.45	0.1	21.9	78.0	1.6	29.4	69.0	41.7	22.4
RPL	1.26	0.3	23.9	75.8	2.5	38.2	59.3	22.6	25.6
RFL	0.58	0.2	23.1	76.7	2.3	33.2	64.5	34.6	27.7
SRL	1.09	0.4	21.7	77.9	3.0	33.9	63.1	25.0	18.7
MAL	0.40	0.1	23.7	76.2	3.9	26.7	69.4	42.3	21.2

Thus the smectite supply decreases progressively from BG to PU and CZ (Table 2).

In the second basin, there is a single source: kaolinized Chon Aike rocks. No smectite contribution is observed and both the kaolinite-to-quartz ratio and microstructure remain quite constant within the Lower Member of the Baqueró Fm. In these deposits, the kaolinite size is finer and crystals do not have well defined borders with a face-to-face arrangement differing from primary kaolins. This picture changes towards the Upper Member, since the CA deposit has a completely different texture, with a higher kaolinite-to-quartz ratio and well-formed, though fine-grained, kaolinite crystals. This change has been attributed to a different provenance of sediments in the Upper Member of Baqueró Fm, particularly to a large pyroclastic supply.

Only one sedimentary deposit was studied in the Chubut district (CH), so no consideration on sedimentary tendencies is possible. However, mineralogical and textural features of CH are clearly similar to those found in primary kaolins, except for an increased kaolinite-to-quartz ratio. The occurrence of degraded kaolinite stacks with some halloysite fibers is ubiquitous, in contrast with the sedimentary clays of the Santa Cruz province.

These geological and mineralogical characteristics suggest that the genesis of Patagonia sedimentary deposits had a strong influence from the proximity of source areas.

5.3. Influence of parent rock composition

In the Chubut province, primary kaolinization involved the pyroclastic Marifil Fm and, in this case, the mineralogy is strongly affected by parent rock composition and texture. Thus in the C60 quarry, IL has a coarse-grained texture with kaolinite stacks and traces of halloysite, RF is deeply altered into halloysite with minor kaolinite and RP seems to be transitional between the IL and RF lithotypes. These compositional and textural differences of alteration products should be attributed to original, distinct characteristics of porosity and mineralogy of pyroclastics. Moreover, in this quarry, small spots of silicification and very fine quartz stockwork structures were found in the fluidal rhyolite (RF) together with some fluid inclusions (temperature of 180 °C) into tiny quartz veins; all these features are attributed to steam-heated water (Hedenquist and Henley, 1985) and some "primary supergene" process in which the temperature and acidity due to hydrothermal steam (Bethke, 1984) could have been superimposed on weathering.

Former isotopic determinations in primary kaolin deposits (Murray and Janssen, 1984) and especially in the C60 quarry (Dominguez and Murray, 1995) together

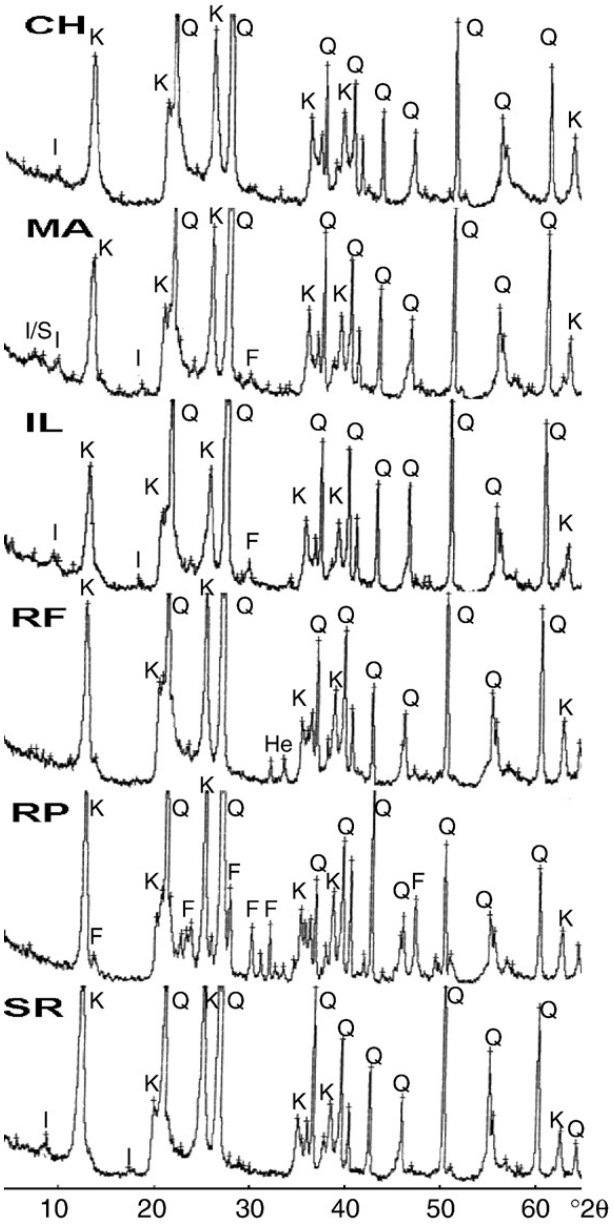

Fig. 10. X-ray diffraction patterns of randomly oriented whole rock clays in the Chubut Province. Q: Quartz, K: Kaolinite, F: Feldespar, I-I/S: Illitic materials.

with new data (Iglesias, 2005) point to a supergene origin linked to meteoric waters. The abundance of halloysite could be somehow connected to this process; an alternative explanation could be the occurrence of different parent phases, since Nagasagua (1969) found that glass had altered to halloysite and biotite to kaolinite. Among the C60 kaolins, RF is the rock with the largest glass content (Iglesias, 2005). This explanation could be also invoked for the SR deposit, which is rich in halloysite, as well as for MA, whose kaolinitic composition could be derived from the alteration of a very fine-grained crystalline tuff. However, the occurrence of illite in MA could be related to a different alteration degree. Interestingly, both grain size and textural characteristics of kaolin MA are similar to those of clay CA in the Santa Cruz province, both thought to have originated in fine-grained crystalline tuffs.

6. Conclusions

Kaolin deposits outcropping in the Chubut and Santa Cruz provinces include primary deposits formed by weathering of Jurassic volcanics (i.e. Bajo Grande, Chon Aike or Marifil Fms) and secondary deposits formed by sedimentation in Cretaceous-Paleocene fluvial–palustrine environments (Baqueró and Salamanca Fms). The origin of primary kaolins is ascribed to weathering in a wet and warm climate based on geological, palaeoclimatic, and geochemical evidence (oxygen and hydrogen isotopes in kaolinite and trace elements). In particular, the elements geochemically linked to gold epithermal mineralizations do not show any concentration increase in primary kaolin blankets. This is also true for the Cantera 60, where some influence of a steam-heated-type hydrothermal alteration may be recognized.

Genesis and compositional features of kaolins are to a large extent comparable in the two districts, the main difference being the prevalence of sedimentary deposits in the Santa Cruz province and of residual kaolins in Chubut. The mineralogical, grain size, and textural characteristics of clays are controlled by parent rock composition (primary kaolins) or by provenance and proximity to source areas (sedimentary clays). The mineralogy of secondary clay deposits reflects both provenance and stratigraphic position. As a consequence, the clays overlying the Bajo Grande Fm consist of smectite and kaolinite in variable proportions, mostly depending on the proximity of the basement. In contrast, where the basin received sediments only from the Chon Aike basement, kaolinite becomes gradually finer upwards, with crystals having more irregular borders reflecting some destruction during erosion and transportation. The deposit pertaining to the Upper Member of the Baqueró Fm does not follow this trend, due to a prevailing pyroclastic supply that fostered the formation of a larger amount of fine-grained but well ordered kaolinite plus some halloysite.

The influence of parent rock composition and texture is observed in the mineralogy and microstructure of primary kaolins: mostly crystalline pyroclastic rocks (e.g. IL and RP) yielded ordered kaolinite arranged in booklets, while lithotypes rich in volcanic glass (e.g. RF and SR) weathered predominantly into halloysite.

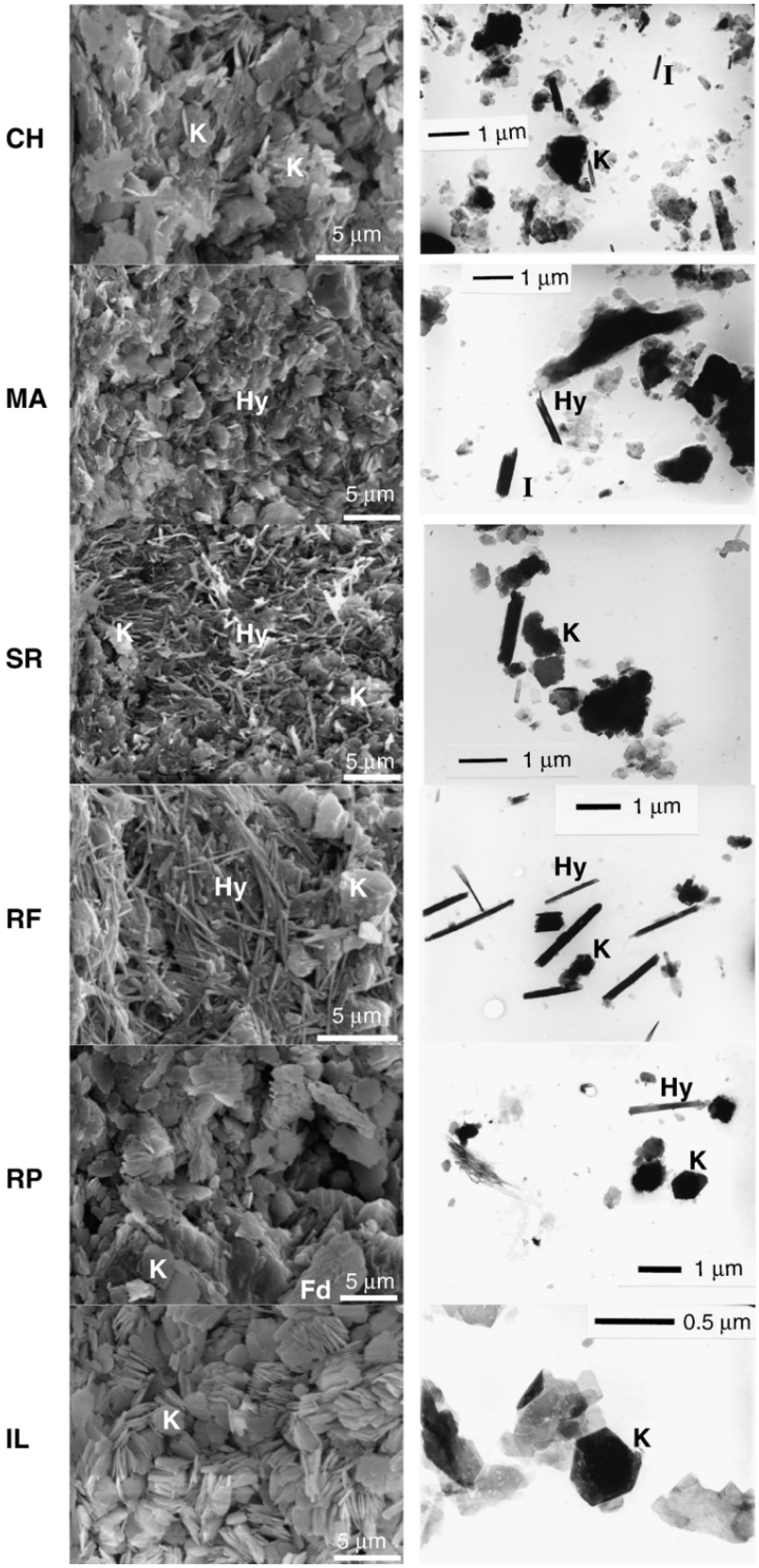

Fig. 11. SEM and TEM micrographs of kaolins from the Chubut Province. K: Kaolinite, Hy: Halloysite, Fd: Feldspar, I-I/S: Illitic materials.

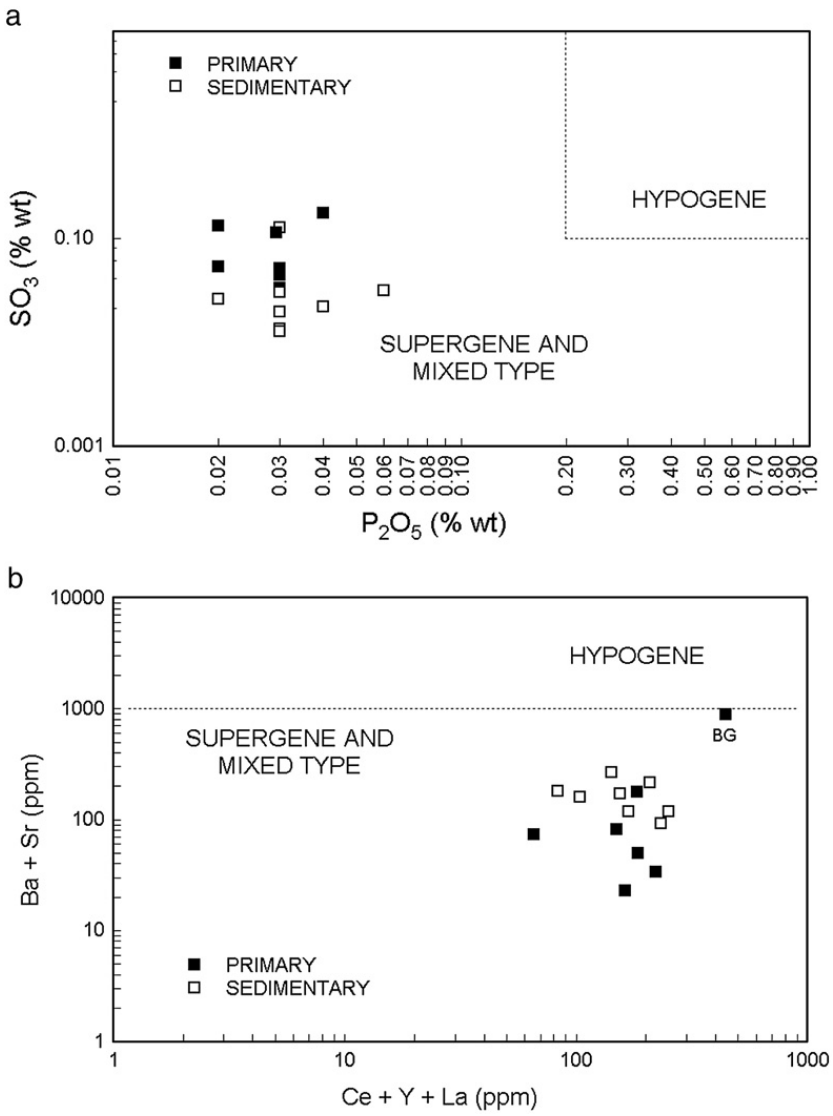

Fig. 12. Binary diagrams discriminating hypogene versus supergene genesis of kaolin deposits (after Dill et al., 1997, 2000). a) P_2O_5 versus SO_3; b) Ce+Y+La versus Ba+Sr.

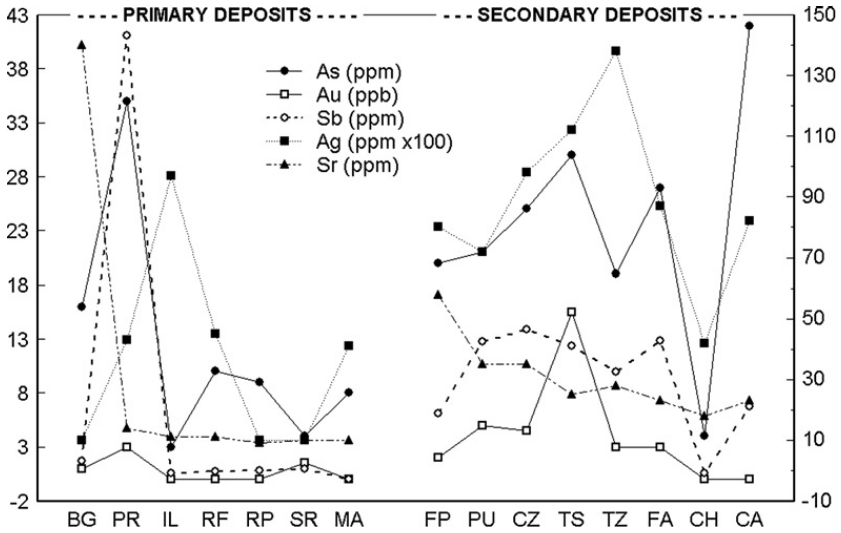

Fig. 13. Distribution of trace elements connected with epithermal events in primary and secondary kaolin deposits from Patagonia.

Acknowledgements

This study was carried out within the framework of the CNR-CONICET 2003-2004 bilateral agreement. Authors are grateful to CNR, CONICET, and Piedra Grande SA for their financial support.

References

Aparicio, P., Galán, E., 1999. Mineralogical Interference on Kaolinite Crystallinity Index Measurements. Clays and Clay Minerals 47, 12–27.

Archangelsky, S., 1959. Estudio geológico y paleontológico del Bajo de la Leona. Acta Geológica Lilloana 2, 5–133.

Archangelsky, S., 1963. Nota sobre la flora fósil de la zona de Ticó, provincia de Santa Cruz. Revista de la Asociación Paleontológica Argentina 3, 57–63.

Archangelsky, S., 1967. Estudio de la Formacion Baqueró, Cretacico inferior de Santa Cruz, Argentina. Revista del Museo de La Plata, Paleontologia 5, 63–171.

Arrondo, O.G., 1972. Estudio geológico y paleontológico en la zona de la Estancia La Juanita y alrededores. Museo de La Plata. Revista (NS). Paleontología 7, 1–94.

Bethke, P.M., 1984. Controls on base and precious-metal mineralization in deeper epithermal environments. U.S. Geological Survey, Open File Report 84-890. 40 pp.

Caranza, H.F., 1988. Estudio estratigráfico y paleoambiental de la Formación Baqueró (Cretácico inferior) en el sector norte del Anfiteatro de Ticó, Departamento Magallanes, provincia de Santa Cruz. MSc thesis, unpublished, Universidad Nacional de Buenos Aires, Argentina, 64 pp.

Cravero, M.F., Dominguez, E., 1992. Kaolin deposits in the Lower Cretaceous Baqueró Formation (Santa Cruz Province, Patagonia, Argentina). J. South American Earth Sciences 6, 223–235.

Cravero, M.F., Dominguez, E., Murray, H.H., 1991. Valores de 18O y D en caolinitas indicadoras de un clima templado-húmedo para el Jurásico superior-cretácico inferior de la Patagonia. Revista Asociación Geológica Argentina 46, 20–25.

Cravero, M.F., Dominguez, E., Iglesias, C., 2001. Genesis and application of the Cerro Rubio kaolin deposit, Patagonia (Argentina). Applied Clay Science 18, 157–172.

De Barrio, R.E., Panza, J.L., Nullo, F.E., 1999. Jurásico y Cretácico del macizo del Deseado, provincia de Santa Cruz. Geología Argentina, Anales 29, Secretaría de Minería de la Nación, SEGEMAR, pp. 511–527.

Dill, H.G., Bosse, H.R., Henning, H., Fricke, A., Ahrendt, H., 1997. Mineralogical and chemical variations in hypogene and supergene kaolin deposits in a mobile fold belt in the Central Andes of Northwestern Peru. Mineralium Deposita 32, 149–163.

Dill, H.G., Bosse, H.R., Kasbohm, J., 2000. Mineralogical and Chemical Studies of Volcanic-Related Argillaceous Industrial Minerals of the Central American Cordillera (Western El Salvador). Econ. Geol. 95, 517–538.

Di Persia, A., 1957. Informe previo al levantamiento geológico en escala 1:100.000 de la zona norte de la provincia de Santa Cruz al sur del Río Deseado. 4a campaña. Yacimientos Petrolíferos Fiscales, unpublished, Buenos Aires, Argentina.

Di Persia, A., 1962. Acerca del descubrimiento del Precámbrico en la Patagonia Extrandina, provincia de Santa Cruz. Primeras Jornadas Geológicas Argentinas, Acta 3, 147–154.

Dominguez, E., Murray, H.H., 1995. Genesis of the Chubut river valley kaolin deposits, and their industrial applications. In: Churchman, G.J., Fitzpatrick, R.W., Eggleton, R.A. (Eds.), Proc. 10th Int. Clay Conference, 1993. CSIRO Publishing, Melbourne, Australia, pp. 129–134.

Dominguez, E., Murray, H.H., 1997. The Lote 8 Kaolin Deposit, Santa Cruz, Argentina. Genesis and paper industrial application. In: Kodama, H., Mermut, A.M., Torrance, J.K. (Eds.), Proc. 11th Int. Clay Conference, Ottawa, Canada, pp. 57–64.

Dondi, M., Iglesias, C., Dominguez, E., Guarini, G., Raimondo, M., 2008. The effect of kaolin properties on their behaviour in ceramic processing as illustrated by a range of kaolins from the Santa Cruz and Chubut provinces, Patagonia (Argentina). Appl. Clay Sci. 40, 143–158.

Eichlin, C., 2001. Geological evaluation of a commercial ball clay deposit. Ceram. Eng. Sci. Proc. 22, 5–18.

Guggenheim, S., Bain, D.C., Bergaya, F., Brigatti, M.F., Drits, V.A., Eberl, D.D., Formoso, M.L.L., Galán, E., Merriman, R.J., Peacor, D.R., Stanjek, H., Watanabe, T., 2002. Report of the Association Internationale pour l'Etude des Argiles (AIPEA) nomenclature committee for 2001: Order, disorder and crystallinity in phyllosilicates and the use of the 'Crystallinity index'. Clay Minerals, 37, 389–393.

Hedenquist, J.W., Henley, R.W., 1985. The importance of CO_2 on freezing-point measurements of fluid inclusions: evidence from active geothermal systems and implications for epithermal ore depositation. Economic Geology 80, 1379–1406.

Henchern, J.J., Homovic, J.F., 1998. Facies y paleoambientes volcaniclásticos en el Nesocratón del Deseado. Boletin de Informaciones Petroleras (BIP), Diciembre, 2–23.

Hinckley, D., 1963. Variability in cristallinity values among the kaolin deposits of the Coastal Palm of Georgia and South Carolina. Clays Clay Miner. 11, 229–239.

Iglesias, C., 2005. Génesis y aplicación industrial de los caolines de la Cantera 60. PhD thesis, Universidad Nacional del Sur, Bahía Blanca, Argentina.

Lesta, P., 1969. Algunas nuevas comprobaciones en la geología de la Patagonia. Anales Cuartas. Jornadas Geológicas Argentinas, Buenos Aires, Argentina, pp. 187–194.

Lesta, P., Ferello, R., 1972. Región extraandina de Chubut y norte de Santa Cruz. In: Leanza, A.F. (Ed.), 1st Symp. Regional Geology of Argentina. Academia Nacional de Ciencias, Córdoba, Argentina, pp. 601–653.

Malvicini, M., Llambías, E., 1974. Geología y génesis del depósito de manganeso de Arroyo Verde, provincia del Chubut. Quinto Congreso Geológico Argentino, Buenos Aires, Argentina, Actas II, pp. 185–221.

Murray, H.H., Janssen, J., 1984. Oxygen isotopes — indicators of kaolin genesis? Proc. of the 27th Int. Geological Congress on Non Metallic Mineral Ores, VNU Science Express, vol. 15, pp. 287–303.

Nagasagua, K., 1969. Kaolin minerals in Cenozoic sedimentation in Central Japan. Proc. Int. Clay Conference, Tokio, Japan, pp. 15–30.

Palma, M.A., 1989. Los eventos geológicos del Macizo del Deseado durante la evolución tectónica del continente Austral. Reunión sobre geotransectas de América del Sur, Mar del Plata, 1-3 de Junio de 1989.

Panza, J.L., Zubía, M., Genini, A., Godeas, M., 1994. Hoja Geológica 4969-II. Tres Cerros. Provincia de Santa Cruz. Geología. Dirección de Minería de la Nación, Boletín 213, Buenos Aires, Argentina, pp. 73–103.

Powell, P.S., 1996. Ball clay basics. American Ceramic Society Bulletin 75, 74–76.

Romero, E., Archangelsky, S., 1986. Early Cretaceous Angiosperm Leaves from Southern South America. Science 234, 1580–1582.

Sacomanni, L., Panza, J.L., 1998. Hoja Geológica 4366-3, Las Plumas. Servicio Geológico Minero Argentino, Instituto de Geología y Recursos Minerales, unpublished.

Schalamuk, I.B., Zubia, M., Genini, A., Fernandez, R.R., 1997. Jurassic epithermal Au–Ag deposits of Patagonia, Argentina. Ore Geology Reviews. Elsevier.

Srodon, J., Eberl, D.D., 1987. In: Bailey, S.W. (Ed.), Illite: in Reviews in Mineralogy, Micas, vol. 13. Mineralogical Society of America, pp. 495–544.

Stipanicic, P.N., Reig, O., 1956. Breve noticia sobre el hallazgo de anuros en el denominado "Complejo Porfírico" de la Patagonia Extrandina, con consideraciones acerca de la composición geológica del mismo. Asociación Geológica Argentina, Revista 10, 215–233.

Stipanicic, P.N., Methol, E.J., 1972. Macizo de Somún Cura. In: Leanza, A.F. (Ed.), Geología Regional Argentina. Academia Nacional de Ciencias, Córdoba, pp. 581–599.

Stoch, L., 1974. Mineraly Ilaste ("clay minerals"). Geological Publishers, Warsaw, pp. 186–193.

Worrall, W.E., 1975. Clays and Ceramic Raw Materials. Applied Science Publishers, London.